Society For Biomaterials

Effect of precursor concentration and spray pyrolysis temperature upon hydroxyapatite particle size and density

Jung Sang Cho,[1] Jeong-Cheol Lee,[2] Sang-Hoon Rhee[1,2]

[1]Interdisciplinary Program of Bioengineering, College of Engineering, Seoul National University, Seoul 152-742, Korea
[2]Department of Dental Biomaterials Science, Dental Research Institute & BK21 HLS Plus, School of Dentistry, Seoul National University, Daehakro 101, Jongno, Seoul 110-749, Korea

Received 22 December 2014; accepted 9 March 2015
Published online 17 April 2015 in Wiley Online Library (wileyonlinelibrary.com). DOI: 10.1002/jbm.b.33406

Abstract: In the synthesis of hydroxyapatite powders by spray pyrolysis, control of the particle size was investigated by varying the initial concentration of the precursor solution and the pyrolysis temperature. Calcium phosphate solutions (Ca/P ratio of 1.67) with a range of concentrations from 0.1 to 2.0 mol/L were prepared by dissolving calcium nitrate tetrahydrate and diammonium hydrogen phosphate in deionized water and subsequently adding nitric acid. Hydroxyapatite powders were then synthesized by spray pyrolysis at 900°C and at 1500°C, using these calcium phosphate precursor solutions, under the fixed carrier gas flow rate of 10 L/min. The particle size decreased as the precursor concentration decreased and the spray pyrolysis temperature increased. Sinterability tests conducted at 1100°C for 1 h showed that the smaller and denser the particles were, the higher the relative densities were of sintered hydroxyapatite disks formed from these particles. The practical implication of these results is that highly sinterable small and dense hydroxyapatite particles can be synthesized by means of spray pyrolysis using a low-concentration precursor solution and a high pyrolysis temperature under a fixed carrier gas flow rate. © 2015 Wiley Periodicals, Inc. J Biomed Mater Res Part B: Appl Biomater, 104B: 422–430, 2016.

Key Words: hydroxyapatite, spray pyrolysis, particle size, concentration, sinterability

How to cite this article: Cho JS, Lee J-C, Rhee S-H. 2016. Effect of precursor concentration and spray pyrolysis temperature upon hydroxyapatite particle size and density. J Biomed Mater Res Part B 2016:104B:422–430.

INTRODUCTION

Among methods for synthesizing ceramic powders, spray pyrolysis provides a relatively easy way to control stoichiometry, purity, and reproducibility. It can also be used as a continuous process, and thus is suitable for mass production. However, it is difficult to control the morphology and size distribution of powders produced by pyrolysis, which are known to depend critically upon processing conditions such as reaction temperature,[1] carrier gas flow rate,[2] the concentration of the precursor solution used, and the strength of the droplet generator. Additionally, it is difficult to achieve highly dense particles due to the evolution of gas by the decomposition of reactants during spray pyrolysis at high temperature.[2]

Hydroxyapatite is a bone grafting material that bonds to bone and not the intervening fibrous tissues. Thus, many processing methods have been developed to synthesize hydroxyapatite powder; spray pyrolysis is one of them, but has been rarely used so far due to its delicate processing methods.[1–7] The biggest problem that must be solved to apply it as a tool for synthesizing hydroxyapatite powder is to achieve small and highly dense particles. Typically, the evolution of gas by the decomposition of reactants during spray pyrolysis hinders particle densification and leads to the production of hollow hydroxyapatite particles. Sodium nitrate,[4] citric acid,[6] and PEG[7] have been used to disintegrate hydroxyapatite aggregates into small particles to increase their sinterability has also been used to densify particles. However, these processes are long, complicated, and show low yield rate.

In this investigation, the effects of the initial concentration of the calcium phosphate precursor solution and of spray pyrolysis temperature upon the size reduction and densification of hydroxyapatite particles were examined, with the primary goal of optimizing these parameters to obtain highly sinterable hydroxyapatite powders.

MATERIALS AND METHODS

Synthesis of hydroxyapatite powders by spray pyrolysis

Single-phase hydroxyapatite powder was synthesized by spray pyrolysis. Calcium phosphate precursor solutions with the Ca/P ratio of 1.67 were prepared by dissolving calcium nitrate tetrahydrate (Aldrich) and diammonium hydrogen phosphate (Aldrich) in deionized water, followed by adding 0.19*M* nitric acid (60%; Aldrich) to dissolve the precipitated hydroxyapatite powders. The concentrations of

Correspondence to: S.-H. Rhee; e-mail: rhee1213@snu.ac.kr
Contract grant sponsor: National Research Foundation of Korea (NRF), Ministry of Education; contract grant number: 2013R1A1A2004752

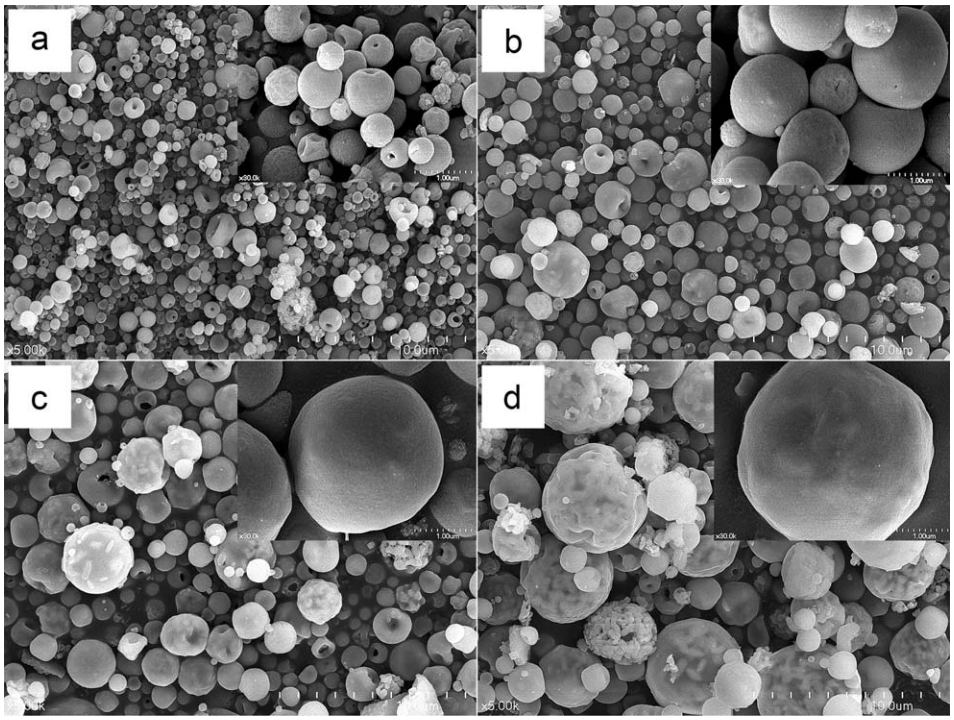

FIGURE 1. FE-SEM images of powders sprayed at 900°C under the air flow rate of 10 L/min, with calcium phosphate precursor solutions of (a) 0.1 mol/L, (b) 0.5 mol/L, (c) 1.0 mol/L, and (d) 2.0 mol/L.

calcium phosphate solutions used in the experiments were 0.1, 0.5, 1.0, and 2.0 mol/L. These precursor solutions were sprayed into an alumina reaction tube with a length of 120 cm and a diameter of 5 cm, at either 900 or 1500°C, and with a carrier gas (air) flow rate of 10 L/min; the apparatus used to generate the spray was a 17-vibrator ultrasonic spray generator with a generating power of 1.7 MHz (Donglim Engineering). Hereafter, hydroxyapatite powders are referred to by abbreviations indicating the temperature and the concentration of the precursor solution used to form them; for example, specimen T900C0.1 refers to the powder formed by pyrolysis at 900°C by spraying 0.1 mol/L calcium phosphate solution. The powders were collected in a Teflon filter placed in the exhaust line of the reactor, which was kept at around 100°C to prevent water condensation.

To evaluate the sinterability of the powders, eight different powders synthesized by using the four different precursor concentrations and the two spray pyrolysis temperatures tested were compacted into disks 10 mm in diameter and 2 mm thick under 20 MPa of pressure, and then were sintered at 1100°C for 1 h in a microwave furnace using the heating rate of 20°C/min.

Characterizations

Microstructures were observed by means of field emission scanning electron microscopy (FE-SEM; S-4700, Hitachi). Crystal phases of specimens before and after sintering were evaluated by means of X-ray diffractometry (XRD; D8 Discover, Bruker). Functional groups of the specimens before and after sintering were analyzed by means of Fourier transform infrared spectroscopy (FTIR; Spectrum 100, Perkin Elmer). For FTIR spectroscopy measurements, pulverized specimens were diluted 250-fold with KBr powder and background noise was corrected by data from pure KBr; 128 scans of each specimen were averaged to yield spectra with 4 cm^{-1} resolution. Relative densities of the sintered specimens were measured by Archimedes' principle.

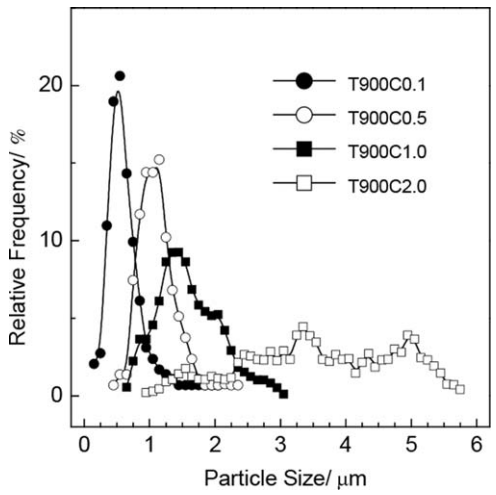

FIGURE 2. Particle size distributions of powders sprayed at 900°C under the air flow rate of 10 L/min, with calcium phosphate precursor solutions of 0.1 mol/L, 0.5 mol/L, 1.0 mol/L, and 2.0 mol/L.

TABLE I. Average Particle Sizes and Particle Size Distributions of the Powders Sprayed at 900°C under the Air Flow Rate of 10 L/min, with Calcium Phosphate Precursor Solutions of 0.1 mol/L, 0.5 mol/L, 1.0 mol/L, and 2.0 mol/L

	Composition			
Characteristics	C0.1	C0.5	C1.0	C2.0
Average particle Size (μm)	0.60 ± 0.29	1.14 ± 0.43	1.53 ± 0.64	3.21 ± 1.59
Particle size distribution (μm)	0.15–2.05	0.45–2.35	0.65–3.05	0.95–5.75

RESULTS

Hydroxyapatite powders prepared by spray pyrolysis at 900°C using the various precursor concentrations were imaged by using FE-SEM (Figure 1); all particles were nearly spherical but had some holes on their outer surfaces. The size of the particles showed depended critically upon on the initial calcium phosphate precursor concentrations; as the precursor concentration was increased, the resulting particle size increased, and the size distribution widened (Figure 2). Table I lists the average particle sizes and the particle size distributions of the specimens prepared by pyrolysis at 900°C; the specimen prepared using the highest initial concentration (T900C2.0) had the largest average particle size and the widest particle size distribution.

XRD patterns were collected of the powders prepared at 900°C using the different precursor concentrations; all specimens were composed of single-phase hydroxyapatite and had low peak intensities and broad full widths at half maximum (FWHM), implying that the powders had poor crystallinity and small grains (Figure 3).

FTIR spectra were collected of the powders prepared at 900°C (Figure 4); in all specimens, the asymmetrical stretching (υ_3) and bending (υ_4) modes of the PO_4 ion were

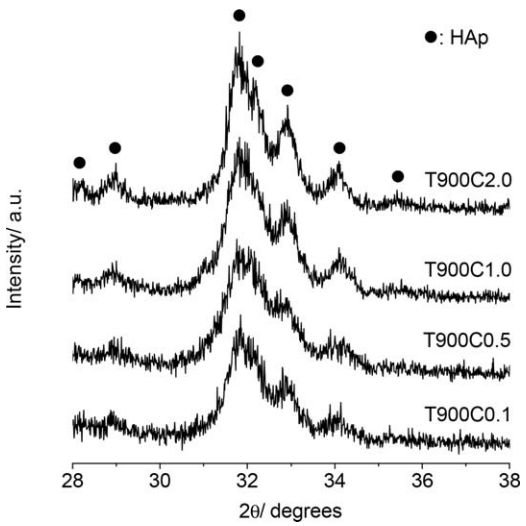

FIGURE 3. XRD patterns of powders sprayed at 900°C under the air flow rate of 10 L/min, with calcium phosphate precursor solutions of 0.1 mol/L, 0.5 mol/L, 1.0 mol/L, and 2.0 mol/L.

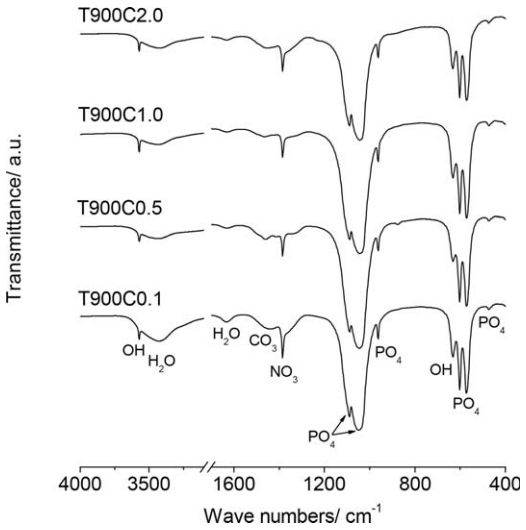

FIGURE 4. FTIR spectra of powders sprayed at 900°C under the air flow rate of 10 L/min, with calcium phosphate precursor solutions of 0.1 mol/L, 0.5 mol/L, 1.0 mol/L, and 2.0 mol/L.

detected at around 1087 and 1046 cm^{-1}, and around 601 and 571 cm^{-1}, respectively.[8] The symmetric stretching modes, υ_1 and υ_2, of the PO_4 ion were detected at around 962 and 474 cm^{-1}, respectively.[8] The stretching and liberation modes of the OH ion were detected at around 3572 and 630 cm^{-1}, respectively.[8] The bands at 1634 and 3435 cm^{-1} were assigned to H_2O deformation and to an envelope of OH groups, respectively. In addition to the bands corresponding to hydroxyapatite, stretching modes of the NO_3 and CO_3 ions were also found at around 1384 and 1457 cm^{-1};[9] these signals arose from residual nitrates in the reactants, such as calcium nitrate tetrahydrate or nitric acid, and from carbonate ions that substituted phosphate sites of the hydroxyapatite.

FE-SEM images were captured of the hydroxyapatite powders prepared by spray pyrolysis at 1500°C (Figure 5); like those prepared at 900°C, the particles in all these specimens were nearly spherical, but they were smaller and denser. Relative to particles prepared by spraying at the lower temperature, noticeably fewer small holes were observed on the outer surfaces of these particles [Figure 5(d)], and the grain sizes were increased. The dependency of particle size upon the precursor concentration was also critical; as the concentration of the precursor solution was increased, the resultant particle size also increased. The size distributions of the powders sprayed at 1500°C were remarkably narrower than those sprayed at 900°C using the same precursor concentrations (Figure 6). Table II lists the average particle sizes and the particle size distributions of the specimens prepared by pyrolysis at 1500°C; the specimen prepared using the greatest initial concentration (T1500C2.0) had the largest average particle size and the widest particle size distribution.

XRD patterns were collected of the powders prepared at 1500°C with different precursor concentrations; all specimens were composed of single-phase hydroxyapatite and had intense peaks with narrow FWHM (Figure 7).

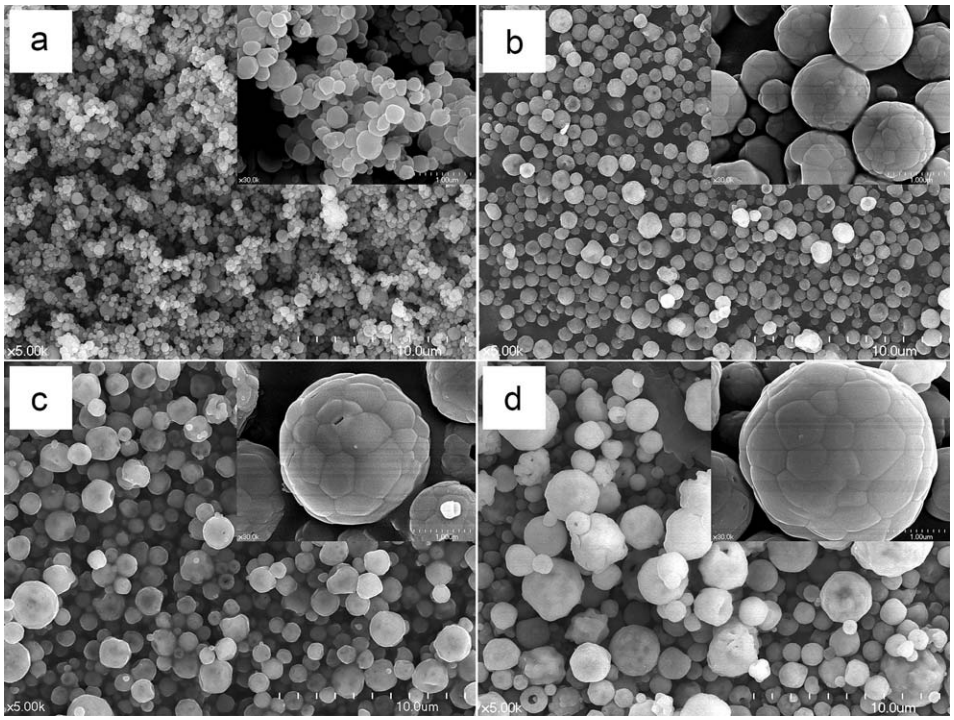

FIGURE 5. FE-SEM images of powders sprayed at 1500°C under the air flow rate of 10 L/min, with calcium phosphate precursor solutions of (a) 0.1 mol/L, (b) 0.5 mol/L, (c) 1.0 mol/L, and (d) 2.0 mol/L.

FTIR spectra were collected of the four as-prepared powders sprayed at 1500°C (Figure 8); in all specimens, the asymmetrical stretching (υ_3) and bending (υ_4) modes of the PO_4 ion were detected at around 1087 and 1046 cm^{-1}, and around 601 and 571 cm^{-1}, respectively.[8] The symmetric stretching modes, υ_1 and υ_2, of the PO_4 ion were also found at around 962 and 474 cm^{-1}, respectively.[8] The stretching and liberation modes of the OH ion were detected at around 3572 and 630 cm^{-1}, respectively.[8] In addition to the bands corresponding to hydroxyapatite, the symmetric stretching modes (υ_3) of the NO_3 ion were also found at around 1384 cm^{-1}.[9] Notably absent was CO_3 band observed in the samples prepared at lower temperature (recall Figure 4).

Hydroxyapatite disks were prepared from the powders prepared at 900°C, and these disks were microwave-sintered at 1100°C for 1 h at the heating rate of 20°C/min; the sintered disks were then fractured for analysis (Figure 9). The grain sizes were similar among these specimens, but the relative sintering density decreased and the number density of pores increased as the precursor concentration increased; Table III lists the sintering densities of these specimens.

XRD patterns were collected of the powders prepared at 900°C and then sintered at 1100°C for 1 h using the heating rate of 20°C/min (Figure 10); all specimens were composed of single-phase hydroxyapatite, and the intensities of their

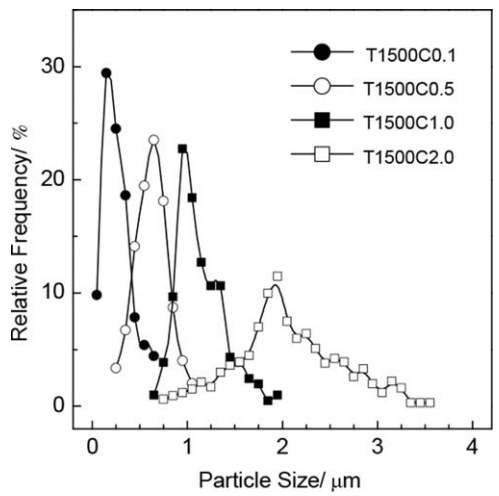

FIGURE 6. Particle size distributions of powders sprayed at 1500°C under the air flow rate of 10 L/min, with calcium phosphate precursor solutions of 0.1 mol/L, 0.5 mol/L, 1.0 mol/L, and 2.0 mol/L.

TABLE II. Average Particle Sizes and Particle Size Distributions of the Powders Sprayed at 1500°C under the Air Flow Rate of 10 L/min, with Calcium Phosphate Precursor Solutions of 0.1 mol/L, 0.5 mol/L, 1.0 mol/L, and 2.0 mol/L

	Composition			
Size and distribution	C0.1	C0.5	C1.0	C2.0
Average particle size (μm)	0.28 ± 0.12	0.63 ± 0.18	1.10 ± 0.30	1.8 ± 0.78
Particle size distribution (μm)	0.05–0.65	0.25–1.05	0.65–1.95	0.75–3.55

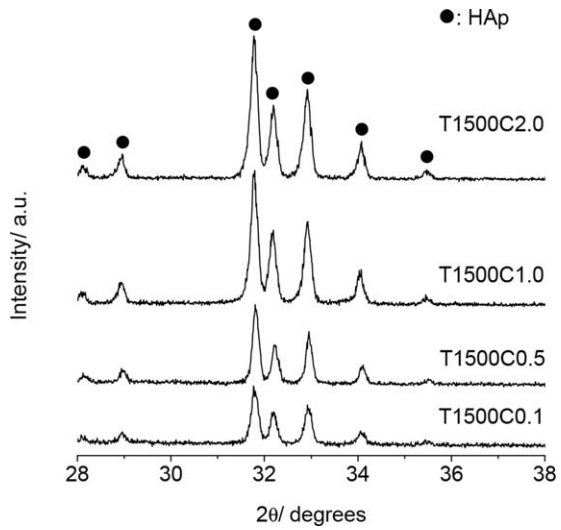

FIGURE 7. XRD patterns of powders sprayed at 1500°C under the air flow rate of 10 L/min, with calcium phosphate precursor solutions of 0.1 mol/L, 0.5 mol/, 1.0 mol/L, and 2.0 mol/L.

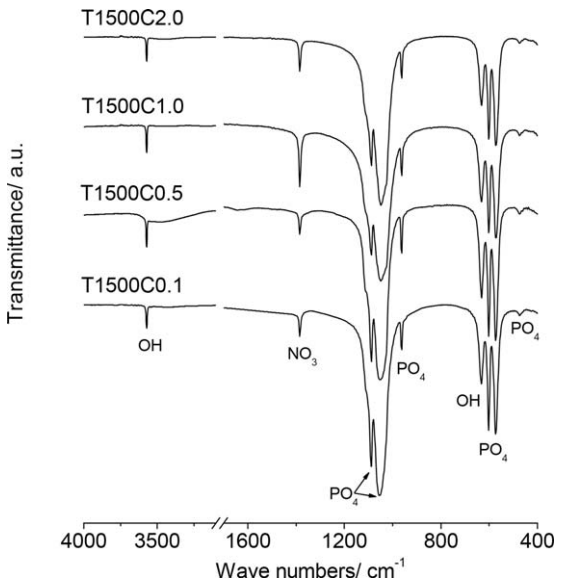

FIGURE 8. FTIR spectra of powders sprayed at 1500°C under the air flow rate of 10 L/min, with calcium phosphate precursor solutions of 0.1 mol/L, 0.5 mol/L, 1.0 mol/L, and 2.0 mol/L.

XRD peaks increased compared to those collected before sintering. FTIR spectra of T900 specimens sintered at 1100°C for 1 h at the heating rate of 20°C/min (Figure 11) showed bands almost identical to those observed for the unsintered powders (recall Figure 4) except for the disappearance of the nitrate and carbonate bands at around 1384 and 1457 cm^{-1}, respectively and development of hydroxide band at around 630 cm^{-1}.

Hydroxyapatite disks were prepared from the powders prepared at 1500°C, microwave-sintered at 1100°C for 1 h at the heating rate of 20°C/min, and then fractured for analysis (Figure 12). The grain sizes were similar among these specimens, but the relative sintering density decreased and the number density of pores increased as the concentration of the precursor solution was increased (Table III).

XRD patterns were collected of the specimens prepared at 1500°C and then sintered at 1100°C for 1 h at the heating rate of 20°C/min (Figure 13); all specimens were

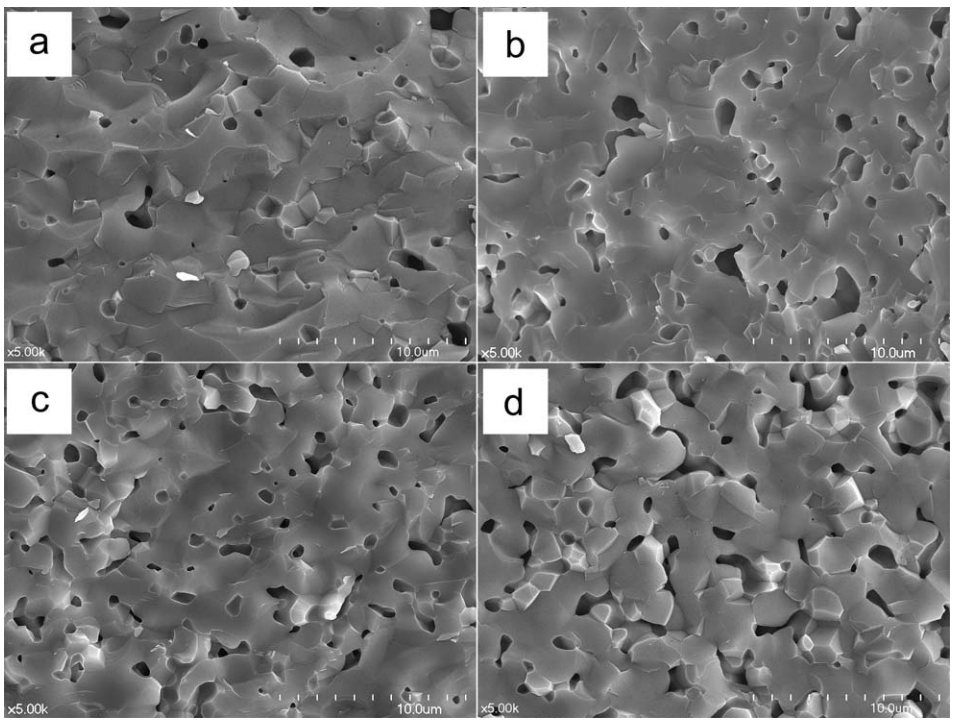

FIGURE 9. Fractured surfaces of microwave-sintered specimens of powders (a) T900C0.1, (b) T900C0.5, (c) T900C1.0, and (d) T900C2.0; sintering was conducted at 1100°C for 1 h using the heating rate of 20°C/min.

TABLE III. Relative Densities of Hydroxyapatite Disks after Sintering at 1100°C for 1 h.

	Composition			
Temperature	C0.1	C0.5	C1.0	C2.0
900°C	94.1 ± 0.3%	92.0 ± 0.3%	89.8 ± 0.4%	86.5 ± 0.5%
1500°C	97.8 ± 0.2%	97.4 ± 0.4%	94.3 ± 0.7%	91.9 ± 0.6%

comprised of single-phase hydroxyapatite, and their peak intensities and FWHM were similar to those collected before sintering. The FTIR spectra of T1500 specimens sintered at 1100°C for 1 h at the heating rate of 20°C/min (Figure 14) showed bands almost identical to those observed for the unsintered powders (recall Figure 8) except for the disappearance of the nitrate band around 1384 cm^{-1}.

DISCUSSION

The dependencies of the size and density of hydroxyapatite particles upon the initial concentration of the calcium phosphate precursor solution and the spray pyrolysis temperature used were examined, using a fixed flow rate of carrier gas. As the initial concentration of the calcium phosphate precursor solution was increased, with a fixed spray pyrolysis temperature and a fixed flow rate of carrier gas, the resultant hydroxyapatite particle size increased. Meanwhile, when the spray pyrolysis temperature was increased, using a fixed precursor concentration and a fixed flow rate of carrier gas, the resultant hydroxyapatite particle size decreased.

Nucleation and growth models of hydroxyapatite crystals based upon the degree of supersaturation in a calcium phosphate droplet, which depends upon the initial concentration of the precursor solution and the spray pyrolysis temperature,[1] are believed to be appropriate for explaining the different size reduction and densification behaviors of hydroxyapatite particles during spray pyrolysis.

The nucleation rate of the hydroxyapatite crystals in the calcium phosphate droplet during spray pyrolysis can be expressed according to the following equation,[10] because heterogeneous nucleation in the droplet cannot occur before homogeneous nucleation of the hydroxyapatite crystals, since there is not yet a nucleation site for it.

$$I = I_0 \exp\left(\frac{-\Delta G^*}{kT}\right) \exp\left(\frac{-\Delta G_m}{kT}\right) \quad (1)$$

Here, ΔG^* is the free energy of the formation of a hydroxyapatite embryo of critical size, ΔG_m is the activation energy for transport across the nucleus–solution interface, and kT has the usual meaning. In Eq. (1), ΔG_m is independent of the specimen, whereas ΔG^* can be expressed by the following equation.

$$\Delta G^* = \frac{16\sigma^3}{\left(\frac{3kT}{V_\beta \ln\left(IP/K_0\right)}\right)^2} \quad (2)$$

Here, σ is the interface energy between the hydroxyapatite nucleus and the solution, IP is the ionic activity product of the hydroxyapatite crystal in the solution, K_0 is the solubility product of the hydroxyapatite, and V_β is the molecular volume of the hydroxyapatite. Formation of the hydroxyapatite from the constituent ions in the solution can be expressed as follows:

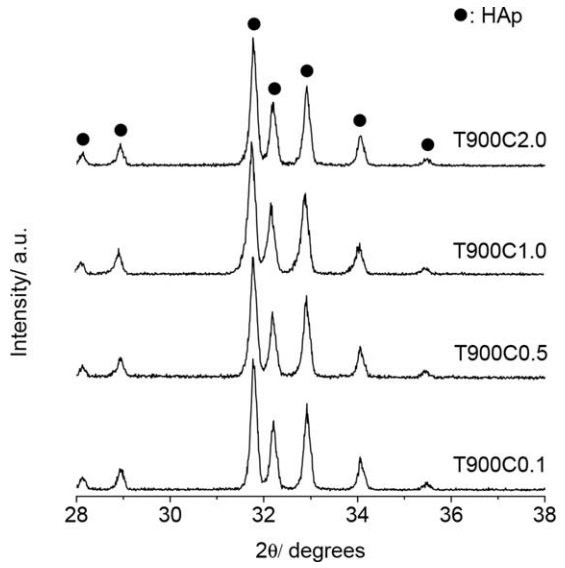

FIGURE 10. XRD patterns of T900 specimens after microwave sintering at 1100°C for 1 h.

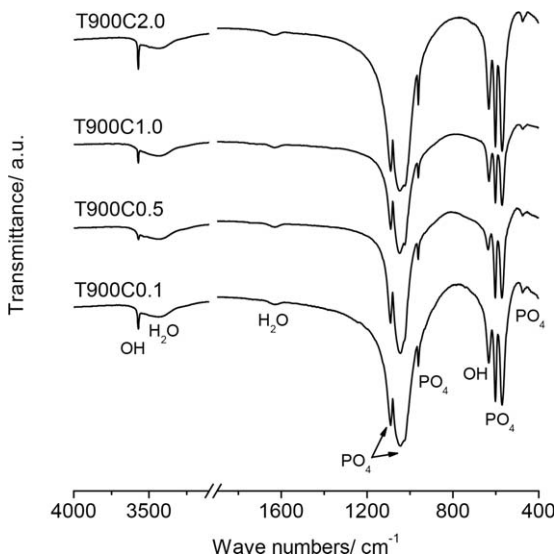

FIGURE 11. FTIR spectra of T900 specimens after microwave sintering at 1100°C for 1 h.

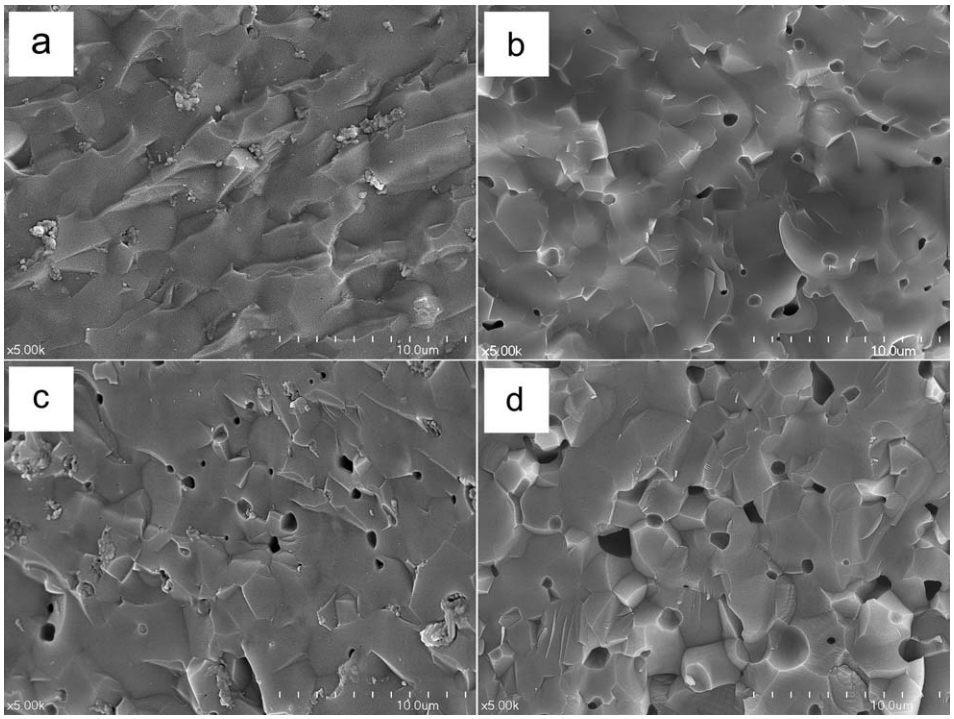

FIGURE 12. Fractured surfaces of microwave-sintered specimens of powders (a) T1500C0.1, (b) T1500C0.5, (c) T1500C1.0, and (d) T1500C2.0; sintering was conducted at 1100°C for 1 h using the heating rate of 20°C/min.

$$10Ca^{2+} + 6PO_4^{3-} + 2OH^- \leftrightarrow Ca_{10}(PO_4)_6(OH)_2 \qquad (3)$$

Therefore, the ionic activity product (*IP*) of hydroxyapatite in the solution can be expressed as follows:

$$\begin{aligned} IP &= (a_{Ca^{2+}})^{10}(a_{PO_4^{3-}})^6(a_{OH^-})^2 \\ &= (\gamma_{Ca^{2+}})^{10}(\gamma_{PO_4^{3-}})^6(\gamma_{OH^-})^2[Ca^{2+}]^{10}[PO_4^{3-}]^6[OH^-]^2 \end{aligned} \qquad (4)$$

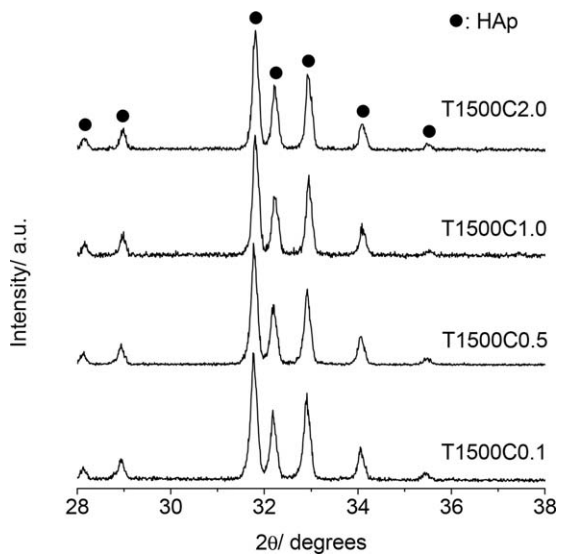

FIGURE 13. XRD patterns of T1500 specimens after microwave sintering at 1100°C for 1 h.

Here, *a* is activity, γ is the activity coefficient, and square brackets represent the concentrations of each ion. The *IP*s of hydroxyapatite in the initial calcium phosphate precursor solution before adding nitric acid (at pH 5.6) were about 10^{-94}, 10^{-86}, 10^{-83}, and 10^{-80} for C0.1, C0.5, C1.0, and C2.0, respectively. Considering that the solubility product (K_0) of hydroxyapatite in aqueous solution is about 5.5×10^{-118} at 37°C,[11] the degrees of supersaturation (IP/K_0) for C0.1, C0.5, C1.0, and C2.0 solutions before adding nitric acid were about 1.8×10^{23}, 1.8×10^{31}, 1.8×10^{34}, and 1.8×10^{37}, respectively. This suggests that the nucleation rate of the hydroxyapatite crystals in the calcium phosphate droplet increased as the concentration of the precursor solution was increased, which means that the number of hydroxyapatite crystals produced in a droplet increased as the precursor concentration was increased.

Besides the increased nucleation rate, relatively longer grain growth was also induced in the droplets as the precursor concentration was increased due to high elemental concentrations of hydroxyapatite, thereby increasing the grain size (Figure 5, inset). The grain size of specimen T1500C0.1 was too small to assess, whereas the average grain sizes of the other three specimens T1500C0.5, T1500C1.0, and T1500C2.0 were about 0.37 ± 0.08 μm, 0.48 ± 0.12 μm, and 0.59 ± 0.19 μm, respectively. The grain sizes of specimens in the T900 series could not be measured due to their small sizes (Figures 1 and 3).

The shrinkage and densification mechanisms of a hydroxyapatite particle when using low and high precursor concentrations under a fixed spray pyrolysis temperature

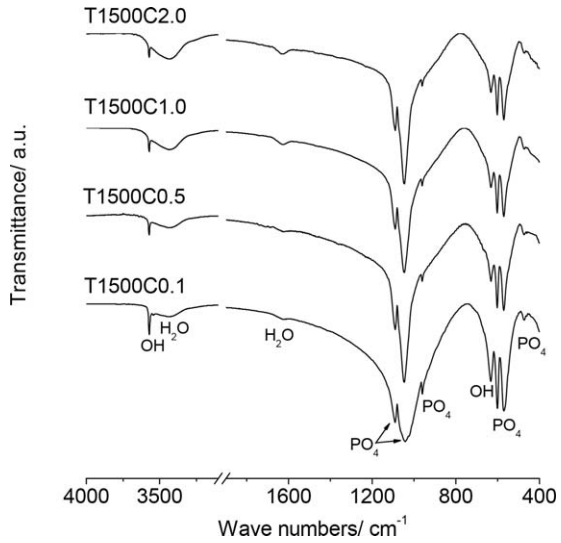

FIGURE 14. FTIR spectra of T1500 specimens after microwave sintering at 1100°C for 1 h.

can be explained based on the above hypotheses. During spray pyrolysis under a fixed temperature, when a calcium phosphate droplet approaches the high-temperature region of the reaction tube, homogeneous nucleation of apatite crystals occurs on the outside of the droplet, while the composition of its interior initially remains unchanged; this occurs because the evaporation of water and nitric acid first increases the local degree of apatite supersaturation near the outer surface of the droplet. As a hydroxyapatite particle, comprising a hydroxyapatite shell (due to homogeneous nucleation and growth of hydroxyapatite crystals at the outer surface of the droplet) surrounding calcium phosphate solution, arrives at the highest-temperature region of the reaction tube, nucleation of hydroxyapatite crystals occurs at the inner surface of the hydroxyapatite shell, followed by growth into the calcium phosphate solution; the nucleation is mainly heterogeneous because heterogeneous nucleation is energetically more favorable than homogeneous nucleation. In this stage, when the initial precursor concentration is low, the number density of newly formed hydroxyapatite nuclei is small and their successive growth is also restricted due to the fast depletion of calcium and phosphate ions in a droplet. This means that the droplet shrinks considerably in size as the water evaporates, due to the low number density and size of the hydroxyapatite crystals formed in the droplet. As a result, the particles obtained after spray pyrolysis are small (Figures 1, 2, 5, and 6).

Contrastingly, when the initial precursor concentration is high, the number density of newly formed hydroxyapatite nuclei is larger, and their subsequent growth continues longer than in droplets with low calcium phosphate concentrations. Thus, less shrinkage from the initial droplet size occurs as the water evaporates, due to the high number density and large size of the hydroxyapatite crystals formed in the droplet. Consequently, the particles formed by spray pyrolysis are larger than those obtained when a low precursor concentration is used (Figures 1, 2, 5, and 6).

Meanwhile, the shrinkage and densification mechanisms of a hydroxyapatite particle when using low and high spray pyrolysis temperature under a fixed precursor concentration can be explained in terms of the dependency of the hydroxyapatite nucleation rate within a droplet upon the evaporation rate of water and nitric acid, as we reported previously.[1] When a high spray pyrolysis temperature is adopted to synthesize hydroxyapatite powder under a fixed precursor concentration, the water and nitric acid in a droplet evaporate quickly, provoking a rapid increase in the ionic activity of hydroxyapatite throughout the droplet. This produces homogeneous nucleation in both the outer and inner regions of the droplet almost simultaneously, thereby inducing considerable shrinkage of each droplet as the water evaporates. Consequently, small and dense hydroxyapatite particles are created (Figure 5).

Contrastingly, when low spray pyrolysis temperature is used to synthesize hydroxyapatite powder, the water and nitric acid in a droplet evaporate first from the outer surface, thereby increasing the local degree of apatite supersaturation near the outer surface of the droplet first, and provoking homogeneous nucleation of apatite crystals, while the composition of its interior initially remains unchanged. As the hydroxyapatite particle, which comprises a hydroxyapatite shell (due to homogeneous nucleation and growth of hydroxyapatite crystals at the droplet's outer surface) surrounding calcium phosphate solution, arrives at the highest-temperature region of the reaction tube, successive heterogeneous nucleation and growth of hydroxyapatite crystals occur at the inner surface of the hydroxyapatite shell, mainly, while some homogenous nucleation also occurs within the droplet. Concurrently, gases originating from the water, nitric acid, and decomposition products of the starting materials in the particle expand due to the high temperature and evaporate instantaneously through the weakest points of the shell, thereby producing holes in the outer surface of the particle (Figure 1). Consequently, large and hollow hydroxyapatite particles with small grain sizes and low crystallinity form because the spray temperature is not high enough to induce homogeneous nucleation and subsequent growth of hydroxyapatite crystals simultaneously throughout the droplet.

The sintering density of hydroxyapatite disks depended critically upon the size and density of their constituent particles, which in turn depended upon the precursor concentration and the spray pyrolysis temperature.[1] The sintering density of hydroxyapatite disks increased as the precursor concentration was decreased, when the spray pyrolysis temperature was fixed; it was also increased by increasing the spray pyrolysis temperature, when the precursor concentration was fixed (Table III). The relationship between the densification rate and the particle size can be expressed as in Eq. (5).[12]

$$\dot{\rho} = \frac{AD}{kTG^m} \tag{5}$$

Here, $\dot{\rho} = \frac{d\rho}{dt}$ is the instantaneous rate of densification, A is an unknown constant that contains the appropriate geometrical and physical parameters, G is the particle size, m is

the scaling law exponent (typically 2 if the densification mechanism is vapor transport, or 4 if the densification mechanism is grain boundary diffusion), and D is the diffusion coefficient. It can be seen from the form of Eq. (5) that the densification rate is proportional to $\frac{1}{G^m}$. This explains the increase of the relative sintering density as particle size is decreased (Table III).

Meanwhile, the relationship between the densification rate and sintering temperature, grain size, and particle density can be expressed as in Eq. (6).[13]

$$\dot{\rho} = B\frac{e^{\frac{-Q}{RT}}}{T}\frac{f(\rho)}{d^n} \tag{6}$$

where $B = \frac{C\gamma V^{\frac{2}{3}}}{R}$. $\dot{\rho} = \frac{d\rho}{dt}$ is the instantaneous rate of densification, d is the grain size, γ is the surface energy, V is the molar volume, R is the gas constant, T is the absolute temperature, Q is the activation energy, $f(\rho)$ is the function of a particle density, C is a constant, and B is a material parameter that is insensitive to d, T, and ρ. As expressed in Eq. (6), the densification rate is proportional to $\frac{f(\rho)}{d^n}$. Therefore, when the grain size in a hydroxyapatite particle increases, the densification rate during sintering decreases. However, the relative sintering densities of T900 specimens, which had smaller grains due to the low spray pyrolysis temperature, were lower than those of T1500 specimens, which had larger grains. This result can be explained in terms of the particle density $[f(\rho)]$ after spray pyrolysis. Particles formed by spray pyrolysis at 900°C were large and hollow spheres with small holes on their outer surfaces, whereas particles formed at 1500°C were small, solid spheres. This result demonstrates that the packing density after molding using T1500 specimens was higher than that using T900 specimens, due to higher particle density [high $f(\rho)$ in Eq. (6)], small particle size, and size distribution, which directly determines the sintering density.[1]

From these results, we can conclude that small and dense particles with high sinterability can be synthesized by using a low concentration calcium phosphate precursor solution and a high spray pyrolysis temperature under a fixed flow rate of carrier gas.[2] When the flow rate of carrier gas is also considered as a processing parameter, the combination of low flow rate of carrier gas,[2] low precursor concentration, and high spray pyrolysis temperature[1] will be advantageous in synthesizing small and solid particles, even though low yield rate will be a drawback.

CONCLUSIONS

The dependency of hydroxyapatite particle size upon the initial concentration of the calcium phosphate precursor solution and upon the spray pyrolysis temperature was examined. The hydroxyapatite particle size increased as the initial concentration of calcium phosphate precursor solution was increased under a fixed spray pyrolysis temperature, and decreased and densified as the spray pyrolysis temperature was increased under a fixed precursor concentration. Sinterability tests showed that the sintering density of a hydroxyapatite disk could be increased by using small and dense hydroxyapatite particles, which could be synthesized by decreasing the initial concentration of calcium phosphate precursor solution and increasing the spray pyrolysis temperature. The practical implication of these results is that highly sinterable hydroxyapatite powders can be synthesized by using a low concentration calcium phosphate precursor solution and a high spray pyrolysis temperature under a fixed flow rate of carrier gas.

REFERENCES

1. Cho JS, Lee J-C, Chung SH, Seo JK, Rhee S-H. Effect of grain size and density of spray-pyrolyzed hydroxyapatite particles on the sinterability of hydroxyapatite disk. Ceram Int 2014;40:6691–6697.
2. Cho JS, Rhee S-H. The densification mechanism of hydroxyapatite particles during spray pyrolysis with variable carrier gas rates of flow. J Biomed Mater Res 2012;100B:493–500.
3. Aizawa M, Hanazawa T, Itatani K, Howell FS, Kishioka A. Characterization of hydroxyapatite powders prepared by ultrasonic spray-pyrolysis technique. J Mater Sci 1999;34:2865–2873.
4. An G-H, Wang H-J, Kim B-H, Jeong Y-G, Choa Y-H. Fabrication and characterization of a hydroxyapatite nanopowder by ultrasonic spray pyrolysis with salt-assisted decomposition. Mater Sci Eng A 2007;449–451:821–824.
5. Kawanobe Y, Honda M, Konishi T, Mizumoto M, Habuto Y, Kanzawa N, Uchino T, Aizawa M. Preparation of apatite microsphere with nano-size pores on the surface via salt-assisted ultrasonic spray-pyrolysis technique and its drug release behavior. J Aust Ceram Soc 2010;46:6–10.
6. Itatani K, Tsugawa T, Umeda T, Musha Y, Davies IJ, Koda S. Preparation of submicrometer-sized porous spherical hydroxyapatite agglomerates by ultrasonic spray pyrolysis technique. J Ceram Soc Jpn 2010;118:462–466.
7. Cho JS, Rhee S-H. Formation mechanism of nano-sized hydroxyapatite powders through spray pyrolysis of a calcium phosphate solution containing polyethylene glycol. J Eur Ceram Soc 2013;33:233–241.
8. Elliott JC. Structure and Chemistry of the Apatites and Other Calcium Orthophosphates. Amsterdam: Elsevier; 1994.
9. Silverstein RM, Bassler GC, Morril TC. Spectrometric identification of organic compounds. New York: Wiley; 1991.
10. Kingery W, Bowen H, Brown D. Introduction to Ceramics. New York: Wiley; 1960.
11. McDowell H, Gregory TM, Brown WE. Solubility of $Ca_5(PO_4)_3(OH)$ in the system $Ca(OH)_2$-H_3PO_4-H_2O at 5, 15, 25, and 37°C. J Res Natl Bur Stand 1977;81A:273–281.
12. Hering C. Effect of change of scale on sintering phenomena. J Appl Phys 1950;21:301–303.
13. Wang J, Raj R. Estimate of the activation energies for boundary diffusion from rate-controlled sintering of pure alumina, and alumina doped with zirconia or titania. J Am Ceram Soc 1990;73:1172–1175.